Frontiers of Physics
https://doi.org/10.1007/s11467-018-0836-5
Front. Phys.
14(1), 13401 (2019)

REVIEW ARTICLE

The art of designing carbon allotropes

Run-Sen Zhang, Jin-Wu Jiang†

Shanghai Institute of Applied Mathematics and Mechanics, Shanghai Key Laboratory of Mechanics in Energy Engineering, Shanghai University, Shanghai 200072, China
Corresponding author. E-mail: †*jwjiang5918@hotmail.com*
Received May 15, 2018; accepted June 18, 2018

Stimulated by the success of graphene and diamond, a variety of carbon allotropes have been discovered in recent years in either two-dimensional or three-dimensional configurations. Although these emerging carbon allotropes share some common features, they have certain different and novel mechanical or physical properties. In this review, we present a comparative survey of some of the major properties of fifteen newly discovered carbon allotropes. By comparing their structural topology, we propose a general route for designing most carbon allotropes from two mother structures, namely, graphene and diamond. Furthermore, we discuss several future prospects as well as current challenges in designing new carbon allotropes.

Keywords carbon allotropes, mechanical properties

Contents

1 Introduction

Carbon is an extremely versatile element with multiple chemical bonding possibilities, resulting in the existence of a large number of carbon allotropes [1]. Graphite and diamond are two classic carbon-based materials. Graphite is a good conductor, and hence, is typically used as a standard electrode [2–5]. Diamond is a well-known superhard material, and is widely used as hard tips in experiments [6–8]. In 1985, C_{60} and other buckyballs were discovered and several novel properties of the buckyballs were explored. After the gold rush for the buckyball, carbon nanotubes have attracted intense research interest since their discovery in 1991. In 2004, single-layer graphene was experimentally obtained for the first time, and has gained considerable attention in the carbon family [9]. Till date, the discovery and study of carbon allotropes have led to several Nobel Prizes, including the discovery of the buckyball C_{60} in 1996 and experiments with graphene in 2010 [9, 10]. There are other proposed structures such as the recently erethynylated dehydroannulenes, expanded radialenes, radiaannulenes [11], sparse fullerene structures [12], conjugated zinc porphyrin nanoball [13], belt-shaped carbon structures [14] and others [15–17].

Carbon allotropes have wide applications in several industrial fields. Graphite, with a reasonably high Li ion capacity and being strong enough to withstand mechanical strains during the insertion process, has been used as an efficient anode material in Li ion batteries produced by SONY [18–20] Diamond, with ultrastrong C-C sp3 bonds, is extremely robust and can be used as a hard tip for vari-

ous indentation experiments [21–24]. Carbon fiber, with a low density and certain advanced mechanical properties, is an important high-quality composite used in the aircraft field [25–28].

Due to the industrial and academic significance of carbon allotropes, there has been increasing interest in recent years in discovering more two-dimensional (2D) carbon allotropes. These newly discovered carbon allotropes have certain different characteristic properties that have been discussed separately in the respective original studies. However, a comparative survey of these new carbon allotropes discovered in the last few years is lacking, and is the focus of the present review. A large number of review articles have been published on the well-studied carbon allotropes, such as buckyballs [10], graphene [29–40], diamond [41–43], carbon nanotubes [44–48]. Hence, we are not going to discuss these well-known carbon allotropes. Instead, we will primarily focus on the 2D and three-dimensional (3D) carbon allotropes explored in the past decade.

In this review, we have presented a comparative survey of the physical and mechanical properties of a variety of carbon allotropes, including seven 2D and eight 3D materials. The results of the comparison, summarized in Tables 2 and 3, will be valuable for further studies on other properties of these carbon allotropes. By analyzing the relationship between the structural topology of these carbon allotropes, we propose a systematic route to synthesize these carbon allotropes by manipulating the carbon atoms or C-C bonds in the two mother structures, graphene and diamond. This theoretical study can facilitate the discovery of new carbon allotropes in a more systematic way.

2 2D semiconductor carbon

Semiconductors play a fundamental role in everyday life and are of key importance for the development of the present electric technique. Several semiconduction 2D carbon allotropes with finite electronic band gaps have been proposed, which will be discussed in this section.

2.1 Graphenylene

Graphenylene, also called biphenylene carbon, was first reported by Balaban *et al.* [62] and was successfully synthesized in the experiment [63, 64]. First-principles simulations proposed to synthesize graphenylene from porous graphene via dehydrogenation [65].

Graphenylene has a lattice structure of P_6/mmm symmetry as shown in Fig. 1A [60]. It is a 2D sp^2-hybridized carbon network with cyclohexatriene unit cells containing twelve carbon atoms. There are three inequivalent C-C bond lengths as listed in Table 1.

Table 1 The C-C bond lengths, unit cell parameters and the diameter of the pores of the optimized structures of previous theoretical predictions

	Ref. [56][a]	Ref. [57][b]	Ref. [58][c]	Ref. [59][d]	Ref. [60][e]	Ref. [61][f]
L_1 (Å)	1.366	1.378	1.371	1.366	1.350	1.367
L_2 (Å)	1.467	1.468	1.472	1.471	1.460	1.473
L_3 (Å)	1.478	1.481	1.478	1,479	1.480	1.474
a (Å)	6.76	6.788	6.72	6.764	6.735	6.760
L_d (Å)	3.2	–	5.51	–	5.47	5.49

[a]DFT GGA-PBEsol;
[b]SIESTA: GGA-PEBsol;
[c]Dmol^3: GGA-PEB;
[d]VASP:GGA-PEB;
[e]CRYSTAL14: hybrid functional;
[f]VASP: GGA-PEB.

Graphenylene is energetically less stable than graphene by about 0.62 eV per atom, but more stable than graphdiyne by about 0.14 eV per atom [66].

The Young's modulus for graphenylene is 648.80 GPa (217.3 N/m) (assuming an effective thickness of 0.335 nm) and the Poisson's ratio is 0.259 [60]. Anisotropic effects were found on mechanical properties for graphenylene nanoribbons [67]. The Young's modulus is 68.31 N/m and 79.42 N/m along the armchair and zigzag directions, respectively. The ultimate strength is 429.43 nN (9.59 N/m) and 1140.59 nN (25.47 N/m) for the armchair and zigzag graphenylene nanoribbons, respectively.

Theoretical results for the electronic band gap of the graphenylene are quite diverse. Small band gaps of 0.025 eV and 0.034 eV have been predicted by two recent works [56, 68], while a band gap of in the range 0.8-1.08 eV were also predicted [60, 69, 70]. The electronic band gap is tunable by hydrogenation and halogenation [59]. Graphenylene in tubal forms have also been studied, and the electronic band gap is about 0.7 eV which can be tuned by axially strain [71].

Graphenylene has been proposed to be efficient gas separators, by taking advantage of its porous configuration. By stretching graphenylene with different strains, it is able to seperate several gases, such as CO_2, N_2, CO, CH_4, or ^3He [56, 58, 61]. The porous nature of the graphenylene enables it to be a promising candidate as anode material for Li ion battery of high mobility and high capacity [66, 72].

2.2 Penta-graphene

Penta-graphene was proposed theoretically by Zhang *et al.* in 2015 [50], which was predicted to be a metastable structure that can undergo phase transition via strain or temperature [73, 74]. Penta-graphene has not been synthesized in the experiment, and may not easy to observe

this material according to the works by Ewels *et al.* [75] The cohesive energy per atom is −7.071 eV [76]. Compared with the cohesive energies of graphene (−7.973 eV/atom), penta-graphene is less stable by about 0.9 eV per atom.

Figure 1B shows the lattice structure of penta-graphene in square unit cell with lattice constant of 3.64 Å. There are six atoms in the unit cell, two C1 carbon atoms and four C2 carbon atoms. Penta-graphene is a closely resembling of the single bond C1-C2 (1.55 Å) and double bond C2-C2 (1.34 Å) [77, 78]. It is a quasi 2D material with buckling height of 1.2 Å. Penta-graphene consists 5-carbon rings, which can be obtained through graphene by the reduction of some C-C bonds.

Mechanical properties of peta-graphene have attracted intense research interest in recent years. As a direct result of the buckling configuration, penta-graphene exhibits a negative Poisson's ratio of −0.068 [50]. The Poisson's ratio can be increased to 0.243 or 0.236 through hydrogenation or fluorination [79]. The in-plane Young's modulus for penta-graphene is about 263.8 GPa·nm (263.8 N/m) in Ref. [50], or 376 N/m in Ref. [80]. Cranford *et al.* predicted the yield strength to be 12.2 N/m at strain 5.1%, while the ultimate strength to be 23.8 N/m at strain 55.8%, and the elastic toughness to be 5.4 J/m^2 [80]. Sun *et al.* obtained similar value of 23.51 N/m for the ultimate strength at strain 0.18 [81]. Hydrogenation, fluorination and the hydroxyl functional groups can efficiently tune a variety of mechanical properties of penta-graphene, including Young's modulus, yield strength, stability, and the buckling height [74, 79, 82, 83].

Penta-graphene has a rather large electronic band gap typically around 3.2 eV [50, 84–87]. Even larger values

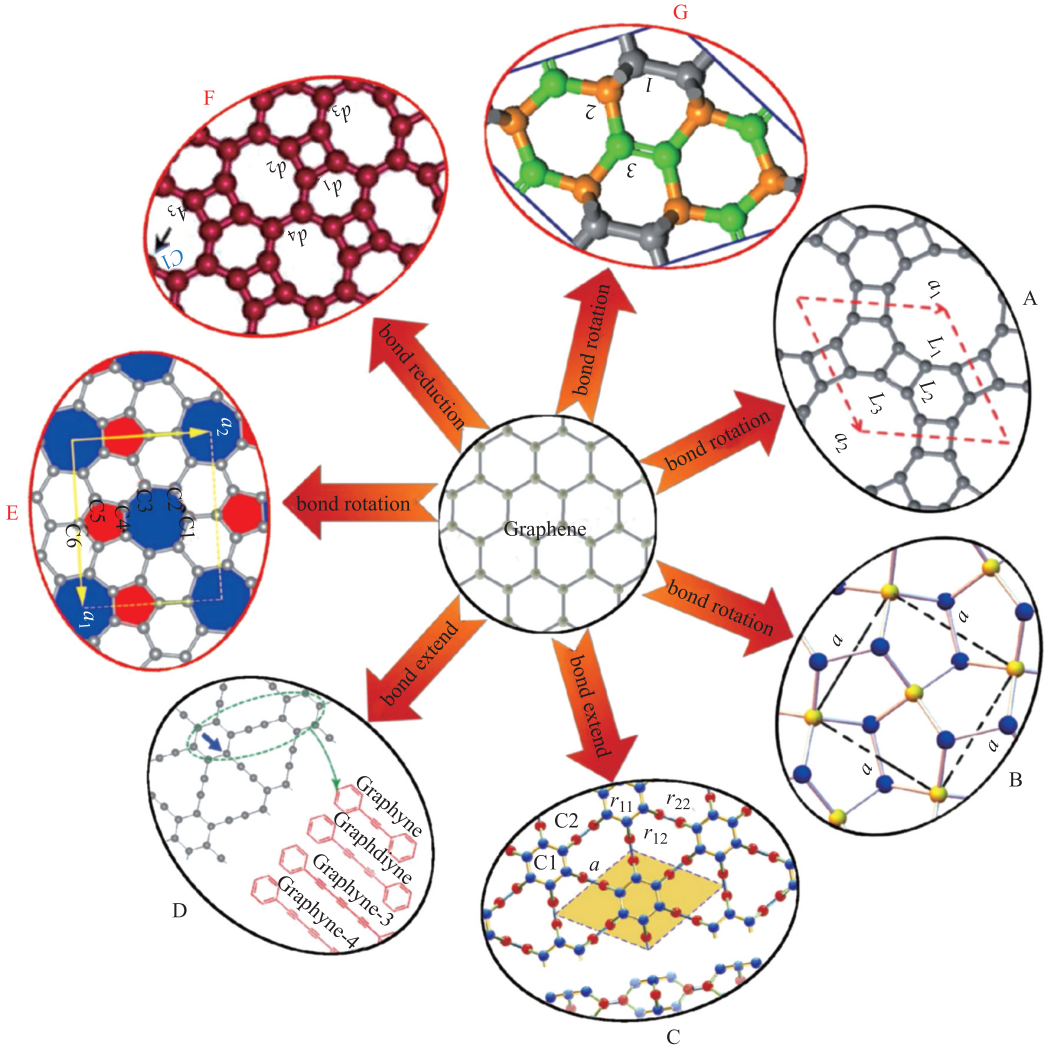

Fig. 1 Carbon allotropes are designed by manipulating the carbon atom or C-C bond in graphene, including the rotation of C-C bonds, the extension of C-C bonds, and the rearrangement of C-C bonds. These carbon allotropes are **(A)** graphenylene [49]; **(B)** penta-graphene [50]; **(C)** twin grapene [51]; **(D)** graphyne [52]; **(E)** phagraphene [53]; **(F)** biphenylene [54]; **(G)** H_{18} carbon [55].

were also predicted for the electronic band gap of penta-graphene, eg., 4.1–4.3 eV [77] or 4.48 eV [76] which are close to the value of insulators. The electronic band gap can be manipulated via various approaches, including stacking style [84], doping or hydrogenation [79, 88, 89], vacancy or Stone–Wales defects [89], and layer number [76]. Penta-graphene in the nanoribbon form was predicted to exhibit some interesting electronic and magnetic properties [90, 91].

Theoretical works have predicted high thermal conductivity for penta-graphene, which is dominately contributed by the phonon transport as the electron thermal conductivity is neglectable due to large band gap. The thermal conductivity at room temperature was predicted to be 167 $W{\cdot}m^{-1}{\cdot}K^{-1}$ [92], 197.85 $W{\cdot}m^{-1}{\cdot}K^{-1}$ [93], 645 $W{\cdot}m^{-1}{\cdot}K^{-1}$ [94], and 350 $W{\cdot}m^{-1}{\cdot}K^{-1}$ [95]. The thermal conductivity is insensitive to the layer number of penta-graphene [96], but it can be tuned through hydrogenation [95] or oxidization [97].

There are some potential applications for penta-graphene owing to its quasi-2D and slightly buckling configuration and the large electronic band gap. Theoretical studies have suggested penta-graphene to be applied as a low-cost catalyst for CO oxidation [98], hydrogen storage [88], and anode material for Li ion battery [99].

2.3 Twin graphene

Twin graphene was proposed theoretically in 2017 through first-principles calculations and MD simulations [51]. There are 18 atoms in the unit cell with two inequivalent carbon atoms C1 and C2 as shown in Fig. 1C, leading to three bond lengths $r_{11} = 1.42$ Å, $r_{12} = 1.55$ Å, and $r_{22} = 1.34$ Å. The lattice structure of the twin graphene can be obtained by substituting the hexagonal carbon ring in the graphyne by a pair of hexagonal carbon rings (see Figs. 1C and D).

From an energetic point of view, a larger cohesive energy means better structural stability. The cohesive energy of twin graphene is smaller than that of graphene by about 0.8–0.9 eV based on different approaches [51].

Twin graphene has an electronic band gap about 1.0 eV depending on the first-principles method, which is very close to the band gap of silicon (1.17 eV), one of the most important industrial semiconducting materials. It is thus expected that the twin graphene is one of the most promising candidates for the electric devices.

Benefit from its "twin" structure, twin graphene inherits some advanced mechanical properties from graphene. For example, the in-plane stiffness is about 186 N/m (20.9 eV/atom), and the Poisson's ratio is 0.32. The bending stiffness 1.39 eV is very close to that of graphene [100]. In particular, twin graphene is able to sustain a large strain of 17% and 16% along the zigzag and armchair directions, respectively. These excellent mechanical properties can support the application of twin graphene in the flexible electric devices.

2.4 Graphyne

The existence of graphyne was conjectured before 1960 [62], and only Graphdiyne has been synthesized in the experiment [101]. A large piece of graphdiyne film was grown on copper [102] and silver substrates [103]. As stimulated by the success in the experiment, lots of theoretical works have been done to explore mechanical, electric, and possible applications for graphyne. There have been some review articles on a variety of properties of graphyne [104–108].

The crystal structure of the graphyne family is shown in Fig. 1D, which displays a flat porous configuration for this material [109, 110]. Note that the length of the carbon chain (acetylene link) connecting two hexagonal carbon rings can be varied, resulting in unlimited number of possible structures in the graphyne family. The four graphyne members with shortest acetylene links are displayed in Fig. 1D, which are called graphyne, graphdiyne, graphyne-3, and graphyne-4. The carbon chain has four carbons for the specific graphyne shown in Fig. 1D. There are four inequivalent carbon-carbon bonds in graphyne, with bond length 1.432, 1.396, 1.233, and 1.339 Å [111].

The maximum binding energies for graphyne and graphdiyne are obtained at 7.95 and 7.78 eV/atom, respectively. While the values are 8.66 eV/atom for graphite and 8.22 eV/atom for fullerene C_{60}, as conpared [112]. The calculated energy [113], E, for graphdiyne is 0.803 eV/atom with respect to graphene, whereas E values for diamond, graphite, (6, 6) nanotube, fullerene C_{60}, and carbyne are −0.022, −0.008, 0.114, 0.364, and 1.037 eV/atom, respectively.

The Young's modulus for the armchair and zigzag directions in graphyne was predicted to be 170.4 N/m and 224.0 N/m by Buehler *et al* [114]. The ultimate stresses along the armchair and zigzag directions for graphyne are 48.2 GPa and 107.5 GPa in Ref. [114], or 14.437 N/m and 20.471 N/m in Ref. [115]. The ultimate strains for the armchair and zigzag directions for graphyne are 0.0819 and 0.1324 in Ref. [114], or 0.112 and 0.177 in Ref. [115]. Peng *et al.* demonstrated the elastic deformation of the graphyne in a wide strain range [116]. Defects are found to be important for various mechanical properties of the graphyne [117]. Graphyne sheet undergos three continuous phase transitions as the timperature increases from 2800 K to 5000 K, where some defects such as 4, 5, 7, 8 and 9-membered rings and large holes start to appear at 1700 K [118].

Due to its porous configuration, the Young's modulus depends on the length of the acetylene link in graphyne members. For instance, Yue *et al.* found that the in-plane stiffness decreases from 166 N/m to 88 N/m with the number of carbon atoms in the acetylene line increasing from

1 to 4 [119]. Similar size dependence was also found in other works [120, 121]. Pei *et al.* found that the in-plane stiffness is 7.60 eV/Å^2 and the Poisson's ratio is 0.453 for graphdiyne, respectively [122]. The ultimate stresses along the armchair and zigzag directions for graphdiyne are 9.538 N/m and 20.835 N/m in Ref. [115]. The ultimate strains for the armchair and zigzag directions for graphyne are 0.109 and 0.208 in Ref. [115].

The graphyne members have intrinsic electronic band gap from 0.46 eV to 1.22 eV depending on the first-principles approaches and the length of the acetylene line [104, 111, 112, 123–125]. The electronic properties can be tuned by hydrogenation [126]. Long *et al.* predicted that the electron mobility and hole mobility for graphdiyne are 2×10^5 cm$^2\cdot$V$^{-1}\cdot$s^{-1} and 2×10^4 cm$^2\cdot$V$^{-1}\cdot$s^{-1}, respectively [127, 128]. Similar results are obtained by Xi *et al.* [129]. The electronic properties for graphyne members can be efficiently tuned via adsorption of transion metal [128] or strain engineering [130].

Taking advantage of their porous structures, recent studies have proposed some possible applications for the graphyne members in fields such as supercapacitors [131], anode materials for lithium batteries [132] or lithium ion battery [133–137], the Li ion storage [138, 139], hydrogen purification [125], catalysts [140, 141], hydrogen production in a photoelectrochemical water splitting cell [142], membrane for hydrogen gas separation [143],

3 2D metallic carbon

3.1 Phagraphene

In 2015, Wang *et al.* [53] proposed phagraphene to be a new stable carbon allotrope, using the systematic evolutionary structure searching. This planar carbon allotrope is energetically comparable to graphene and more favorable than other carbon allotropes proposed in previous works due to its sp^2-hybridization and dense atomic packing. While it has not been snthesized in lab. The total energy of phagraphene is calculated to be −9.03 eV/atom. Compared with graphene (−9.23 eV/atom), phagraphene is less stable by just 0.2 eV/atom [53].

The structure of phagraphene is shown in Fig. 1E with Pmg space group, which is constructed by 5-6-7 carbon rings. From the structural point of view, this structure can be derived from graphene by rotating a C-C bond in the 6-carbon ring. There are five inequivalent C-C bonds in phagraphene with bond length of 1.52 Å (C1–C6), 1.44 Å (C2–C3), 1.41 Å (C3–C4), 1.43 Å (C4–C5), and 1.40 Å (C5–C6) [53].

The elastic modulus of phagrphene is calculated to be 870±15 GPa (291.5±5 N/m) along the armchair direction and 800 ± 14 GPa (268 ± 5 N/m) along the zigzag direct (assuming an effective thickness of 0.335 nm). And the tensile strength of phagraphene is predicted to be around 85 ± 2 GPa, independent of loading direction [144]. The Young's modulus is 292.9 N/m and the Poisson's ratio is 0.255 for phagraphene [81]. The ultimate tensile strength is 25.39 N/m at the strain of 0.18 and 25.57 N/m at the strain of 0.16 in the armchair and zigzag directions, respectively [81]. The mechanical properties for phagraphene can be tuned by hydrogenation or fluorination [145].

Phagraphene has a special electronic band structure with distorted Dirac cones, and these Dirac cones are robust against external strain [146]. Phagraphene is a conductor with zero band gap. The electronic band gap can be opened through hydrogenation and fluorination, which can induce band gaps of 4.29 eV and 3.23 eV for the fully hydrogenation and fluorination, respectively [145]. The electronic band structure for the phagraphene nanoribbon can be manipulated by B-, N-, and BN-doping [147], or free edges [148, 149].

The thermal conductivity is found to be anisotropic with 218±20 W$\cdot$m$^{-1}\cdot$K^{-1} and 285±29 W$\cdot$m$^{-1}\cdot$K^{-1} along the armchair and zigzag directions, respectively [144]. First-principles calculations predict phagraphene to be a promising candidate for anode materials in Li ion battery, with higher mobility and Li ion storage capacity [150].

3.2 Biphenylene

Biphenylene was first synthesized by Lothrop in 1941, which is a planar configuration containing 4-, 6-, and 8-carbon rings [151]. As shown in Fig. 1F, we can obtain the structure from graphene by rotating two C-C bonds in the 6-carbon ring to get the 4- and 8-carbon rings. there are two types of carbon atoms in biphenylene, with C1 from the 4-carbon ring and C2 from other carbon rings. These two types of atoms form four different C-C bond lengths in biphenylene, i.e., 1.458 Å, 1.454 Å, 1.407 Å, and 1.447 Å, and four different bond angles.

The total energy of biphenylene is calculated to be −8.82 eV/atom and the corresponding volues for graphene and phagraphene are −9.28 and −9.08 eV/atom, respectively. So biphenylene is only 0.47 eV/atom less stable than graphene. Biphenylene is even stable upto a high temperature of 5000 K [73].

The Young's modulus is 613±35 GPa (205.4±11.7 N/m) and 716 ± 45 GPa (239.9 ± 15.1 N/m) along the armchair and zigzag, respectively (assuming an effective thickness of 0.335 nm) [73]. Yedla *et al.* found that the Young's modulus is as large as 3.4 TPa (1139 N/m) along the armchair direction, and is 652 GPa (218.4 N/m) in the zigzag direction [152]. The ultimate stress is 138 GPa at strain 0.064 for the armchair direction, and 23 GPa at strain 0.15 for the zigzag direction [152].

First-principles calculations have predicted biphenylene to be metallic [153], and biphenylene nanotubes are also metallic, irrespective to their chiralities [154]. The biphenylene nanoribbons of zigzag edges are also metal-

lic, while biphenylene nanoribbons with armchair terminations have finite electronic band gap that decreases with increasing ribbon width [153]. The electronic and excitonic optical absorption properties have also been investigated for the biphenylene [155]. The electronic band gap for biphenylene can be opened by hydrogenation or fluorination, and a metal to insulator transition was realized by full hydrogenation [154].

Biphenylene has a large Li ion storage capacity and high Li ion mobility [150]. Furthermore, the volume expansion during the Li insertion is about 11%. These properties enable biphenylene to be a suitable candidate for the anode of Li ion battery. Biphenylene also has a reasonablly large capacity for the storage of hydrogen [156].

4 3D metallic carbon

Owing to the outstanding properties of metallic carbon as well as their great potential applications, design and synthesis of three-dimensional metallic carbons are currently one of the hot issues.

4.1 H_{18} carbon

H_{18} carbon was proposed by Zhao *et al.* by first-principles calculations in 2015 [55]. This 3D lattice essentially consists of covalently bonded graphene layers, so the configuration of H_{18} carbon can be regarded as a derivative from the graphene as shown in Fig. 1G. This new carbon allotrope has not been synthesized in the experiment, but it may exist in recent detonation experiment as revealed by the XRD simulation [164]. It is a metallic carbon allotrope with 3D sp^2-sp^3 hybridized bonding network structure in the P6/mmm (D^1_{6h}) symmetry as shown in Fig. 1G. We can obtain the structure through graphene by bond rotation. The lattice parameters are $a = b = 7.125$ Å and $c = 2.605$ Å. There are three inequivalent carbon atoms, forming four bond lengths: 1.591, 1.631, 1.475, and 1.317 Å. The density of H_{18} carbon is 3.135 g/cm^3.

The cohesive energy is 8.75 eV/atom, so H_{18} carbon is energetically stable. There is no imaginary frequency in the phonon dispersion, which implies the thermal stability for H_{18} carbon. The stability of H_{18} carbon is further verified by computing the independent elastic constants, which satisfy the Born stability condition [165]. The bulk modulus and shear modulus of H_{18} carbon are 360 GPa and 361 GPa, respectively.

4.2 Hex-C_{18}

Hex-C_{18} is a 3D metallic carbon allotrope that was proposed by Liu *et al.* with the global structure search [157]. Although this new carbon allotrope has not been synthesized in the experiment, XRD calculations have provided some clues for the existance of Hex-C_{18} in detonation soot [164, 166]. Figure 2A shows the hexagonal lattice structure for Hex-C_{18} with space group P6$_3$/mcm (D^3_{6h}). We can also obtain the structure through graphene by some bonds rotations. There are 18 atoms in the unit cell, which are categrized into the sp^3 hybridized carbon C_1 and sp^2 hybridized carbon C_2. The lattice constants are $a = b = 8.36$ Å and $c = 2.46$ Å. Hex-C_{18} is a porous structure with low density of 2.41 g/cm^3.

The bulk modulus and shear modulus for Hex-C_{18} are 282.9 GPa and 254.6 GPa, respectively. The Vickers hardness of Hex-C_{18} was predicted to be 42.2 GPa with Chen's model [167] or 80.8 GPa with Gao's model [168], so Hex-C_{18} is a superhard material. Hex-C_{18} was suggested to be a possible anode material, with low Li diffusion energy barriers and high specific capacity.

4.3 Tri-C_9

In 2016, Wen *et al.* proposed a new 3D metallic carbon allotrope termed as Tri-C_9, by distorting the sp^3 hybridization bond in the diamond structure [158]. This carbon allotrope has not been verified experimentally, but simulations suggested that it is possibe to produce Tri-C_9 by compressing graphite at pressure above 70 GPa. The lattice structure for Tri-C_9 is shown in Fig. 2B, which has the R32 (No.155) space group. The lattice constants are $a = b = 4.083$ Å and $c = 3.848$ Å, respectively. The bond lengths are 1.526 Å and 1.528 Å, which are close to each other. The six bond angles in tetrahedron of Tri-C_9 are 60°, 105.778°, 105.778°, 122.944°, 122.944°, and 123.807°, which are substantially different from that of diamond (109.5°), indicating the distortion of sp^3 bonds in Tri-C_9.

The stability of Tri-C_9 was supported by examing the phonon dispersion and the elastic constants. There is no imaginary frequency in the full phonon dispersion at ambient pressure, so Tri-C_9 is thermaldynamically stable. The independent elastic constants satisfy the mechanical stability criteria, which further suggests the mechanical stability of Tri-C_9.

First-principles calculations have also predicted some mechanical properties for Tri-C_9. The bulk modulus and shear modulus for Tri-C_9 are 365 GPa and 272 GPa, respectively. The Vickers hardness according to the model by Chen [167] is 34.8 GPa.

4.4 O-type and T-type carbon

In 2017, Liu *et al.* proposed a series of carbon allotropes by self-assembling ultrathin diamond nanostripes, termed O-type and T-type carbon [159]. Figure 2C shows the configuration for two sampling structures. The allotrope is orthorhombic (Cmmm) or tetragonal (P4$_2$/mmc) corresponding to the odd or even number of diamond nanostripes that are assembled. The allotrope of orthorhombic

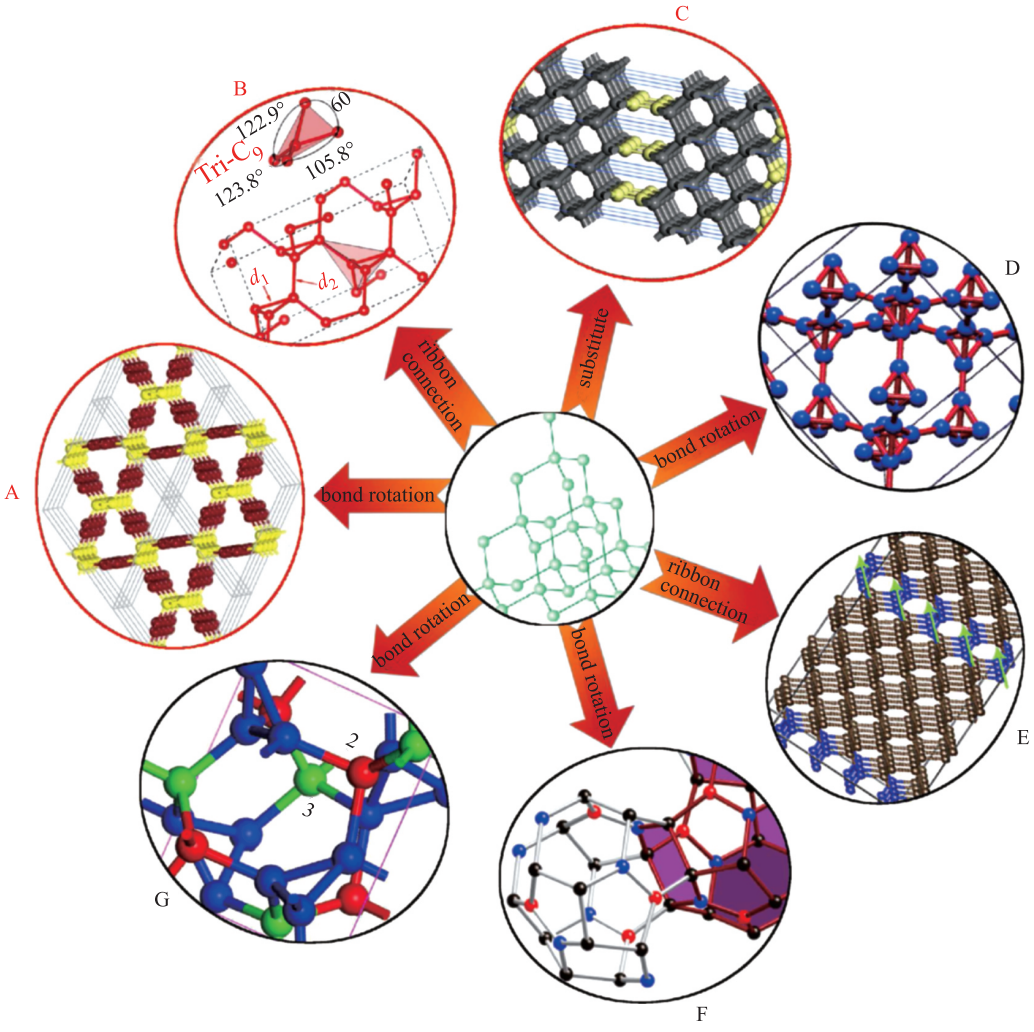

Fig. 2 The design of carbon allotropes based on diamond through a verity of manipulations: the rotation of C-C bonds in diamond, the substitution of carbon atom by clusters, or the combination of small diamond segments. The carbon allotropes are **(A)** Hex-C_{18} [157]; **(B)** tri-C_9 [158]; **(C)** O-type and T-type carbon [159]; **(D)** T-carbon [160]; **(E)** C_{14}-diamond [161]; **(F)** tetragonal C_{64} [162]; **(G)** C_{20}-T carbon [163].

symmetry is called O-type carbon, while the allotrope of tetragonal symmetry is called T-type carbon. T10 carbon was found in the experiment [169]. The thermal and mechanical stability of the O-type and T-type carbons were confirmed by examining phonon dispersions and elastic constants. The cohesive energies of these two allotropes are larger than some other carbon allotropes, like the T-carbon [160]. A distinct feature for the T-type and O-type carbons is their superhard property that is inherit from diamond.

5 3D superhard carbon

There has been a long-standing search for 3D metallic, superhard carbon, stable under ambient conditions.

5.1 T-carbon

T-carbon was predicted theoretically in 2011 by Sheng *et al.* [160] and has been synthesized in the experiment in 2017 [170]. It is a semiconductor with electronic band gap 2.25 eV or 2.968 eV [160]. As shown in Fig. 2D, T-carbon can be regarded as a derivative of the diamond structure by substituting each carbon atom by a carbon tetrahedron. The resultant lattice constant is 7.52 Å and the equilibrium density is 1.5 g/cm^3. The cohesive energy per atom is predicted to be 6.573 eV.

The bulk and shear modulus of T-carbon are 169 GPa and 70 GPa, respectively [160]. Gao *et al.* [168] found that T-carbon is a superhard material with hardness of 61.1 GPa, while Chen *et al.* [171] predicted the hardness to be less than 10 GPa.

Due to its low density, T-carbon may be used for hydro-

gen storage, with the gravimetric and volumetric hydrogen capacities around 7.7 wt% and 0.12 kg H_2/L, respectively [160]. In the meantime, the thermal conductivity of T-carbon is about 33.06 $W{\cdot}m^{-1}{\cdot}K^{-1}$, which is much lower than the value of 2388.69 $W{\cdot}m^{-1}{\cdot}K^{-1}$ for diamond, because the interaction within T-carbon is weaker than diamond [172].

5.2 C_{14}-diamond

In 2017, Wu *et al.* performed first-principles calculations to predict C_{14}-diamond [161]. It is a derivative structure from the diamond as shown in Fig. 2E, and has many similar properties as diamond. For instance, the cohesive energy for C_{14}-diamond is 8.983 eV/atom, which is very close to the cohesive energy of diamond, so C_{14}-diamond is thermodynamical stable. The stability of this structure was also confirmed by the generalized elastic stabiliity criteria with nin independent elastic constants. The density of C_{14}-diamond is 3.37 g/cm^3, also very close to the density of diamond. C_{14}-diamond is a superhard material with hardness of 55.8 GPa.

5.3 Tetragonal C_{64}

In 2016, Wei *et al.* proposed a new semiconductor with band gap of 1.32 eV – tetragonal C_{64}. [162]. This carbon allotrope has a tetragonal symmetry (space group $I4_1/amd$ No. 141) as shown in Fig. 2F. The lattice constants are $a = 7.1801$ Å and $c = 9.6649$ Å for the tetragonal unit cell. The density of tetragonal C_{64} is 2.562 g/cm^3. The stability of the tetragonal crystal is verified using the criteria for the mechanical stability [173] with six independent elastic constants. Furthermore, the there is no imaginary frequency for the phonon dispersion over the whole Brillouin zone, indicating the dynamical stability of tetragonal C_{64}.

According to the model by Lyakhov *et al.* [174], the hardness for tetragonal C_{64} is 60.2 GPa, so it is a superhard material. But the hardness is 34.0 GPa from the model by Chen *et al.* [167]. The Young's modulus is 510 GPa and the Poisson's ratio is 0.178. The bulk modulus B and the shear modulus G are 264 GPa and 217 GPa within the Voigt–Reuss–Hill approximation, so the B/G ratio is 1.22. This B/G ratio is lower than 1.75, indicating a brittle character [175]. The weakest tensile strength is 48.1 GPa in the [111] direction, while the strongest tensile strength is 78.8 GPa in the [110] direction. The lowest shear strength is 48.2 GPa in the (100)[010] direction and the highest shear strength is 60.1 GPa in the (111)[-1-12] direction.

5.4 C_{20} T-carbon

Using first-principles calculations, Wang *et al.* proposed the structure for C_{20} T-carbon and discussed its stability [163]. It is an insulator with electronic band gap of 5.44 eV. The structure of C_{20} T-carbon is shown in Fig. 2G, which has a space group $P2_13$ (No. 198). The lattice constant is 4.495 Å. There are twenty carbon atoms in the primitive unit cell with three inequivalent carbon atoms, resulting in four different C-C bond length: 1.541 Å, 1.548 Å, 1.550 Å, and 1.541 Å.

C_{20} T-carbon was predicted to be stable, as there is no imaginary frequency in the whole phonon dispersion. The stability of C_{20} T-carbon is also verified by computing these three independent elastic constants in cubic lattice, which satisfy the Born stabiligy condition. The bulk and shear modulus is 395 GPa and 427 GPa according to the Voigt–Reuss–Hill approximation. The B/G ratio 0.93 is lower than 1.75, so C_{20} T-carbon is brittle. The Poisson's ratio of C_{20} T-carbon is 0.11. One advanced property for C_{20} T-carbon is its high hardness of 72.76 GPa, so this is a superhard material. The weakest tensile strength of C_{20} T-carbon is about 71.1 GPa in the ⟨110⟩ direction and The lowest shear strength of C_{20} T-carbon is 54.5 GPa.

5.5 P-carbon

Recently, P-carbon was proposed by Pan *et al.* using the evolutionary partical swarm structural search approach [183]. It is a semiconductor with direct band gap of 3.52 eV [183]. We can design new carbon allotropes from not only graphene and diamond but also carbon nanotube. P-carbon can be obtained by compressing large-diamenter single-walled carbon nanotubes, and the stability of the structure has been verified theoretically [173]. Figure 3 shows the configuration of P-carbon, which has a tetragonal symmetry (space group I4/mmm, No. 139) with lattice parameters $a = 11.11$ Å and $c = 2.5$ Å.

The average bond length is 1.54 Å. As a result of the microporous structure, P-carbon has a low density of 3.1 g/cm^3 [183]. P-carbon is stable at high pressure and can be even more stable than graphite at pressure above 115 GPa [183].

The bulk moduli for P-carbon is 334.2 GPa, while the shear moduli is 360.1 GPa. Specifically, P-carbon is a su-

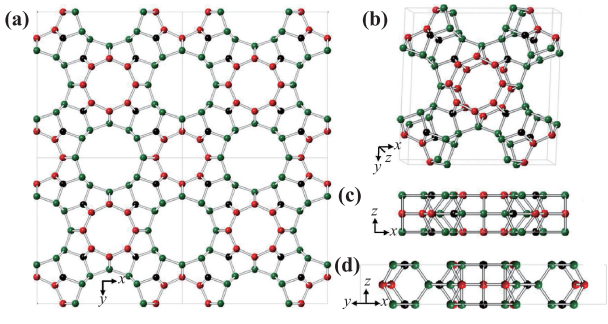

Fig. 3 **(a)** 2×2×1 configuration of P carbon, **(b–d)** Crystal structure of P carbon unit cell and side views along the [0 1 0] and [1 1 0] directions, respectively

perhard material with hardness predicted to be 86.7 GPa. The tensile strengths along [001], [100], and [110] directions are 109.33 GPa at strain 0.32, 37.39 GPa at strain 0.24 and 42.46 GPa at strain 0.24, respectively [183].

6 Future prospects and summary

6.1 Searching for more carbon allotropes

6.1.1 Theoretical design of more carbon allotropes

By comparing the structural topology of existing carbon allotropes in the above, we have learn how to design new carbon allotropes by manipulating the elemental structures (carbon atoms or C-C bonds) in the two most fundamental carbon materials – graphene and diamond. The derivative structure typically inherits the dimensionality of the mother structure; i.e., allotropes derived from graphene (diamond) are always in 2D (3D) configuration. New carbon allotropes can be predicted in a systematic way along this line with the assistance of the first-principles calculations. For example, Enyashin and Ivanovskii have systematically designed twelve 2D carbon allotropes based on graphene by extending the primitive unit cell [17].

In particular, it is possible to construct more complex structures by recursively using this designing technique. As an example, the twin-graphene can be theoretically regarded as the covalent sticking of two graphene single layers. Repeating this twin process will yield a new structure with a finite thickness about four-fold of the thickness of graphene. As a result, the theoretical designing technique can lead to endless carbon based allotropes.

6.1.2 More experimental studies needed

Sometimes, new allotropes are first observed in the experiment and then analyzed theoretically, such as the discovery of C_{60} buckyball. Several decades ago, it is still a challenge for theoreticalists to imagine the exact atomic structure of a newly discovered allotrope. For example, Kroto and heath made a great effort to figure out the novel structure of the buckyball C_{60} [10]. However, with the fast development of the observation techniques, nowadays it is able to examine the structure of new materials on the atomic level, so it becomes an easier task for theoreticalists to determine the actual configuration of the new allotrope after it is synthesized in the labotory.

On the other hand, theoreticalists are now capable to design new carbon allotropes in a systematic manner, mainly thanks to the increase of the computational speed and the fast development of the first-principles calculations approach. Many carbon allotropes of novel imaginary configurations have been predicted theoretically. A key challenge for these predicted carbon allotropes is the experimental verification, because there are usually lots of different allotropes in the product of the experiment. One successful example is the T-carbon, which was first predicted theoretically in 2011 and verified experimentally in 2017. More experiments are needed to verify the theoretical predictions of these new carbon allotropes.

6.2 Properties and applications of carbon allotropes

The properties and applications of each carbon allotrope were discussed separately in original works, which have been summarized in Tables 2 and 3. We have compared most fundamental properties for carbon allotropes in this review, which can facilitate a comparative investigation for possible applications of these carbon allotropes. The first meaningful task is to complete these blank fields in Table 2 by examining these properties that have not been studied.

Another important direction is to compare properties or applications for these carbon allotropes. For instance, most 2D carbon allotropes are proposed to be good electrode materials for the Li ion battery. A natural question arises: who is the best? A systematic study is needed to address such questions.

Furthermore, 2D materials are usually stacked into finite-thickness functional devices in practical applications. Some 2D carbon allotropes have quite different electronic and optical properties, and these varying physical properties can be integrated by stacking in the vertical van der Waals heterostructure form. This stacking technique will lead to the creation of full carbon multi-functional devices.

6.3 Summary

We have summarized some major properties discussed in the present review in Tables 2 and 3. There are general features that can be extracted from the comparison of some properties listed in these tables. Carbon allotropes can be obtained from the two most fundamental carbon materials – graphene and diamond, by manipulating the elemental structures (carbon atoms or C-C bonds); eg., bond rotation, bond extension, or bond reduction for 2D allotropes. More specifically, phagraphene, biphenylene and graphenylene have the lowest relative energy to graphene, and they are obtained through bond rotation. Graphynes and twin graphene can be obtained through the bond extension, which have the medium energy. The pentagraphene is obtained through the bond reduction, which has the highest energy. According to the cohesive energy of these 2D allotropes, the bond rotation is the most feasible manipulation energetically while bond reduction is the most unfeasible.

There is a strong correlation between the Young's modulus and the density of the 2D allotropes in Table 2; i.e., the Young's modulus is linearly proportional to the

Table 2 The comparison of some major physical properties for 2D carbon allotropes discussed in the present review article.

	Graphenylene	Penta-graphene	Twin-graphene	Graphyne family		Phagraphene	Biphenylene
				Graphyne	Graphdiyne		
Density (10^{-7}g/cm^2)	0.6043	0.7521	0.9789	0.5830	0.4629	0.7409	0.7000
Young's moduli (N/m)	217.35 [60];	263.80 [50, 79]	186.00 [51]; 172.00 [51]	162.00 [176]; 166.30 [119]	123.10 [119]; 122.00 [122]	292.90 [81]	205.40 ± 11.70; 239.90 ± 15.10 [73]
Ultimate strength (N/m)		23.80 [80]; 23.51 [81]		14.43 (Armchar) 20.47 (Zigzag) [115]	9.54 (Armchair) 20.84 (Zigzag) [115]	25.39, 25.57, 24.80 [81]	
Poisson's ratio	0.259 [60];	−0.068 [50]	0.32	0.429 [176] 0.416 [119]	0.453 [122] 0.446 [119]	0.255 [81]	
Relative energy (eV/atom)	0.62 [66]; 0.632 [68] 0.66 [57]	0.90 [76]	0.80–0.90 [51]	0.71 [112]	0.80 [113]	0.20 [53]	0.47 [73]
Electronic band (eV)	0.03 (GGA-PBEsol) [56]; 0.034 (PEB) [68] 0.03 (ab initio global search) [68]; 0.83 (periodic DFT) [60]; 0.80–1.08 (density functional tight-binding) [69, 70]	3.27 (HSE06) [84]; 2.29 (PEB) 3.21 (HSE06) [85]; 2.23 (PEB) 3.24 (HSE06) [86]; 2.27 (PEB) 3.25 (HSE06) [50, 87]; 3.27 (HSE06) 4.48 (GW_0) [76]; 4.10–4.30 (GGA-RPBE) [77]	0.98 (FP-LDA-DZ); 0.96 (FP-GGA-DZ); 0.76 (FP-LDA-DZP); 0.73 (FP-GGA-DZP) [51]	1.20 (MNDO) [52]; 0.52 (FP-LCAO) [112]; 0.79 [123]; 0.46 (GGA-PBE) 0.96 (HSE06) [177]; 0.47 (GGA-PBE) 2.23 (Crystal06: B3LYP) [178] 0.47 (VASP) [179]	0.53 (FP-LCAO) [112]; 0.52 (GGA-PBE) 1.18 (Crystal06: B3LYP) [178]; 1.10, 0.44 [124]; 1.22 (hybrid exchange-correlation functional) [125]; 0.44 (ABINIT-YAMBO:LDA), 1.10 (ABINIT-YAMBO:GW) [124] 0.48 (GGA-PBE) [111]; 0.46 (VASP-PAW: GGA-PBE) [127]; 0.53 (CASTEP: GGA-PBE) [180]	metallic (PBE and HSE06) [145]	metallic (GGA-PEB) [73] metallic (GGA-PEB/HSE) [153] metallic (Gaussian: HSEH1PBE/6-31G*) [154]
Thermal conductivity ($Wm^{-1}K^{-1}$)		645 [94]; 198 [93]; 167 [92]; 350 [95]	9 [51]			218 ± 20 (armchair), 285 ± 29 (Zigzag) [144]	
Synthesized or not	Yes [63, 64]	No	No	No	Yes [101–103]	No	Yes [151]
Application	gas separation [56, 58, 61]; li ion battery [66, 72]	catalyst for CO oxidation [98]; hydrogen storage [88]; NO adsorption [181]; Li/Na-ion battery [99]	electric optical devices [51]	lithium batteries [132]; catalyst for hydrogen desorption and sorption [140]; sodium storage [182]	supercapacitor electrode [131]; lithium batteries [131, 133–136, 138, 139]; hydrogen purification [125]; catalyst [140, 141]; lithium capacitor [137]; hydrogen production [142]; gas separation [143]; sodium storage [182]	lithium ion battery [150]	lithium ion battery [150]; hydrogen adsorption [156]

Table 3 A summary of some major properties for 3D carbon allotropes discussed in this review.

	Density (g/cm^3)	E_{coh} (eV/atom)	Bandgap (eV)	Bulk muduli (GPa)	Shear muduli (GPa)	B/G	Hardness (GPa)	Synthesized or not
H18-carbon [55]	3.25 (LDA), 3.14 (PEB)	8.547 (LDA), 7.269 (PEB)	metallic (GGA-PBE/HSE06)	360	361	1.00	–	No
Hex-C_{18} [157]	2.41 (PEB)	7.70 (PEB)	metallic (GGA-PBE/HSE06)	283	255	1.11	42.2 (chen); 80.8 (gao)	No
Tri-C_9 [158]	3.23 (LDA)	7.994 (LDA) 6.86 (PEB) [157]	metallic (LDA/HSE06)	365	272	1.34	34.8 (chen)	No
C_{14}-diamond [161]	3.37	8.983	metallic (GGA-PBE/HSE06)	404	375	1.08	55.8 (chen)	No
P carbon [183]	3.10(LDA)	–	3.52 (HSE06)	334	360	0.93	86.7 (gao)	No
T-carbon [160]	1.50 (GGA); 1.54 (LDA)	6.573 (PEB), 7.503 (LDA)	2.25 (GGA) 2.22 (LDA)	169	70	2.41	less than 10.0 (chen); 61.1 (gao)	Yes [170]
Tetragonal C_{64} [162]	2.56 (PAW)	0.285 (PAW) (relative to diamond)	1.32 (VASP)	264	217	1.22	33.9 (chen) 60.2 (Lyakhov)	No
C_{20}-T carbon [163]	3.41 (LDA); 3.30 (PEB)	8.321 (LDA), 7.191 (PEB)	5.44 (HSE06)	395	427	0.93	72.8 (chen)	No

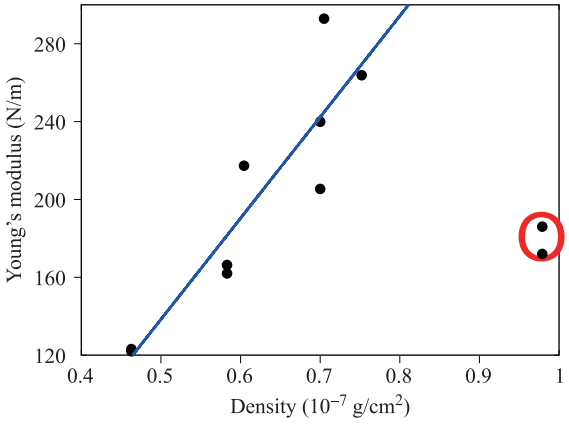

Fig. 4 The Young's modulus versus the density of the 2D carbon allotropes. Data for twin-graphene is enclosed by the circle (red online). The line (blue online) is guide to the eye.

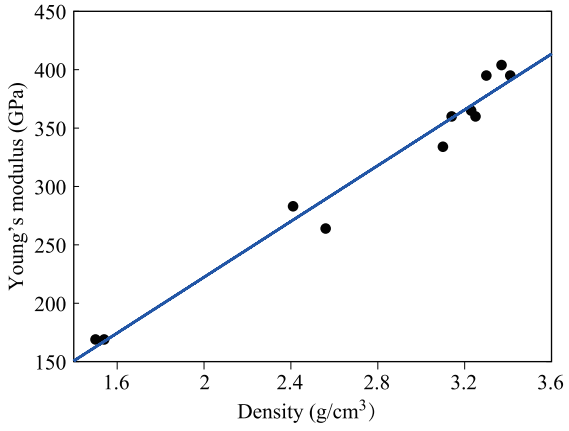

Fig. 5 The Young's modulus versus the density of the 3D carbon allotropes. The line (blue online) is guide to the eye.

density as displayed in Fig. 4. Note that twin graphene deviates from the correlation, because the twin graphene essentially has two layers in the out-of-plane direction. In other words, twin graphene is not an ideal 2D allotrope. Similar correlation is also found for the 3D carbon allotropes listed in Table 3; i.e., the Young's modulus and Shear modulus are both linearly proportional to the density of the material as displayed in Figs. 5 and 6. The phenomenon of increasing modulus (E) with increasing density (ρ) has also been found in other materials, like the bones [184], where the power factor (α) varies in different models $E \propto \rho^{\alpha}$. According to Figs. 4, 5 and 6, the power factor is $\alpha = 1.0$ for the 2D and 3D carbon allotropes.

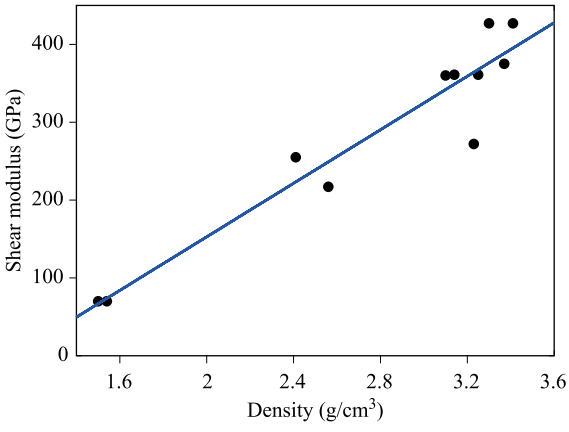

Fig. 6 The Shear modulus versus the density of the 3D carbon allotropes. The line (blue online) is guide to the eye.

Acknowledgements The work was supported by the Recruitment Program of Global Youth Experts of China, the National Natural Science Foundation of China (NSFC) under Grant No. 11504225, and the Innovation Program of Shanghai Municipal Education Commission under Grant No. 2017-01-07-00-09-E00019.

References

1. R. Hoffmann, A. A. Kabanov, A. A. Golov, and D. M. Proserpio, *Homo Citans* and carbon allotropes: For an ethics of citation, *Angew. Chem. Int. Ed.* 55(37), 10962 (2016)
2. A. E. Cass, G. Davis, G. D. Francis, H. A. O. Hill, W. J. Aston, I. J. Higgins, E. V. Plotkin, L. D. Scott, and A. P. Turner, Ferrocene-mediated enzyme electrode for amperometric determination of glucose, *Anal. Chem.* 56(4), 667 (1984)
3. D. Aurbach, B. Markovsky, I. Weissman, E. Levi, and Y. Ein-Eli, On the correlation between surface chemistry and performance of graphite negative electrodes for Li ion batteries, *Electrochim. Acta* 45(1–2), 67 (1999)
4. J. F. Rusling and A. E. F. Nassar, Enhanced electron transfer for myoglobin in surfactant films on electrodes, *J. Am. Chem. Soc.* 115(25), 11891 (1993)
5. D. Aurbach, B. Markovsky, A. Shechter, Y. Ein-Eli, and H. Cohen, A comparative study of synthetic graphite and Li electrodes in electrolyte solutions based on ethylene carbonate-dimethyl carbonate mixtures, *J. Electrochem. Soc.* 143(12), 3809 (1996)
6. M. Lichinchi, C. Lenardi, J. Haupt, and R. Vitali, Simulation of Berkovich nanoindentation experiments on thin films using finite element method, *Thin Solid Films* 312(1–2), 240 (1998)
7. R. Saha, Z. Xue, Y. Huang, and W. D. Nix, Indentation of a soft metal film on a hard substrate: Strain gradient hardening effects, *J. Mech. Phys. Solids* 49(9), 1997 (2001)
8. J. Cao, Y. Wu, D. Lu, M. Fujimoto, and M. Nomura, Material removal behavior in ultrasonic-assisted scratching of SiC ceramics with a single diamond tool, *Int. J. Mach. Tools Manuf.* 79, 49 (2014)
9. K. S. Novoselov, A. K. Geim, S. V. Morozov, D. Jiang, Y. Zhang, S. V. Dubonos, I. V. Grigorieva, and A. A. Firsov, Electric field effect in atomically thin carbon films, *Science* 306(5696), 666 (2004)
10. H. W. Kroto, J. R. Heath, S. C. O'Brien, R. F. Curl, and R. E. Smalley, C_{60}: Buckminsterfullerene, *Nature* 318(6042), 162 (1985)
11. F. Diederich and M. Kivala, All-carbon scaffolds by rational design, *Adv. Mater.* 22(7), 803 (2010)
12. C. Hug and S. W. Cranford, Sparse fulleryne structures enhance potential hydrogen storage and mobility, *J. Mater. Chem. A* 5, 21223 (2017)
13. J. Cremers, R. Haver, M. Rickhaus, J. Q. Gong, L. Favereau, M. D. Peeks, T. Claridge, L. M. Herz, and H. L. Anderson, Template-directed synthesis of a conjugated zinc porphyrin nanoball, *J. Am. Chem. Soc.* 140(16), 5352 (2018)
14. E. Estrada and Y. Sim'on-Manso, Escherynes: Novel carbon allotropes with belt shapes, *Chem. Phys. Lett.* 548, 80 (2012)
15. A. Kochaev, A. Karenin, R. Meftakhutdinov, and R. Brazhe, 2D supracrystals as a promising materials for planar nanoacoustoelectronics, *J. Phys.: Conf. Ser.* 345, 012007 (2012)
16. E. Belenkov and I. Shakhova, Structure of carbinoid nanotubes and carbinofullerenes, *Phys. Solid State* 53(11), 2385 (2011)
17. A. N. Enyashin and A. L. Ivanovskii, Graphene allotropes, *physica status solidi (b)* 248, 1879 (2011)
18. J. B. Goodenough, Evolution of strategies for modern rechargeable batteries, *Acc. Chem. Res.* 46(5), 1053 (2013)
19. Z. Ogumi and H. Wang, Carbon Anode Materials, Springer, 2009
20. D. H. Doughty, Materials issues in lithium ion rechargeable battery technology, *Sampe Journal* 32, 75 (1995)
21. K. McElhaney, J. Vlassak, and W. Nix, Determination of indenter tip geometry and indentation contact area for depth-sensing indentation experiments, *J. Mater. Res.* 13(05), 1300 (1998)
22. A. Richter, R. Ries, R. Smith, M. Henkel, and B. Wolf, Nanoindentation of diamond, graphite and fullerene films, *Diamond Related Materials* 9(2), 170 (2000)
23. W. Ni, Y. T. Cheng, and D. S. Grummon, Microscopic superelastic behavior of a nickel-titanium alloy under complex loading conditions, *Appl. Phys. Lett.* 82(17), 2811 (2003)
24. D. J. Sprouster, S. Ruffell, J. E. Bradby, J. S. Williams, M. N. Lockrey, M. R. Phillips, R. C. Major, and O. L. Warren, Structural characterization of B-doped diamond nanoindentation tips, *J. Mater. Res.* 26(24), 3051 (2011)
25. C. Soutis, Fibre reinforced composites in aircraft construction, *Prog. Aerosp. Sci.* 41(2), 143 (2005)
26. U. Meier, Strengthening of structures using carbon fibre/epoxy composites, *Constr. Build. Mater.* 9(6), 341 (1995)
27. C. Soutis, Carbon fiber reinforced plastics in aircraft construction, *Mater. Sci. Eng. A* 412(1–2), 171 (2005)
28. D. Chung, Carbon materials for structural self-sensing, electromagnetic shielding and thermal interfacing, *Carbon* 50(9), 3342 (2012)
29. N. Song, X. Gao, Z. Ma, X. Wang, Y. Wei, and C. Gao, A review of graphene-based separation membrane: Materials, characteristics, preparation and applications, *Desalination* 437, 59 (2018)
30. A. D. Oyedele, C. M. Rouleau, D. B. Geohegan, and K. Xiao, The growth and assembly of organic molecules and inorganic 2D materials on graphene for van der Waals heterostructures, *Carbon* 131, 246 (2018)
31. J. W. Jiang, Graphene versus MoS_2: A short review, *Front. Phys.* 10(3), 287 (2015)

32. F. Meng, H. Wang, F. Huang, Y. Guo, Z. Wang, D. Hui, and Z. Zhou, Graphene-based microwave absorbing composites: A review and prospective, *Compos. Part B Eng.* 137, 260 (2018)
33. M. Ye, Z. Zhang, Y. Zhao, and L. Qu, Graphene platforms for smart energy generation and storage, *Joule* 2, 245 (2017)
34. A. Darbandi, E. Gottardo, J. Huff, M. Stroscio, and T. Shokuhfar, A review of the cell to graphene-based nanomaterial interface, *JOM* 70(4), 566 (2018)
35. M. J. Allen, V. C. Tung, and R. B. Kaner, Honeycomb carbon: A review of graphene, *Chem. Rev.* 110(1), 132 (2010)
36. V. Singh, D. Joung, L. Zhai, S. Das, S. I. Khondaker, and S. Seal, Graphene based materials: Past, present and future, *Prog. Mater. Sci.* 56(8), 1178 (2011)
37. A. A. Balandin, Thermal properties of graphene and nanostructured carbon materials, *Nat. Mater.* 10(8), 569 (2011)
38. F. Schwierz, Graphene transistors, *Nat. Nanotechnol.* 5(7), 487 (2010)
39. F. Bonaccorso, Z. Sun, T. Hasan, and A. Ferrari, Graphene photonics and optoelectronics, *Nature Photon.* 4, 611 (2010)
40. A. K. Geim, Graphene: Status and prospects, *Science* 324, 1530 (2009)
41. Y. V. Pleskov, Electrochemistry of diamond: A review, *Russ. J. Electrochem.* 38(12), 1275 (2002)
42. O. Auciello and A. V. Sumant, Status review of the science and technology of ultrananocrystalline diamond (UNCD™) films and application to multifunctional devices, *Diamond Related Materials* 19(7–9), 699 (2010)
43. J. P. Goss, Theory of hydrogen in diamond, *J. Phys.: Condens. Matter* 15(17), R551 (2003)
44. J. N. Coleman, U. Khan, W. J. Blau, and Y. K. Gun'ko, Small but strong: A review of the mechanical properties of carbon nanotube–polymer composites, *Carbon* 44(9), 1624 (2006)
45. Q. Cao and J. A. Rogers, Ultrathin films of single-walled carbon nanotubes for electronics and sensors: A review of fundamental and applied aspects, *Adv. Mater.* 21(1), 29 (2009)
46. W. Bauhofer and J. Z. Kovacs, A review and analysis of electrical percolation in carbon nanotube polymer composites, *Compos. Sci. Technol.* 69(10), 1486 (2009)
47. J. Wang, Carbon-nanotube based electrochemical biosensors: A review, *Electroanalysis* 17(1), 7 (2005)
48. O. Breuer and U. Sundararaj, Big returns from small fibers: A review of polymer/carbon nanotube composites, *Polym. Compos.* 25(6), 630 (2004)
49. J. M. Schulman and R. L. Disch, A theoretical study of large planar [*n*]phenylenes, *J. Phys. Chem. A* 111(39), 10010 (2007)
50. S. Zhang, J. Zhou, Q. Wang, X. Chen, Y. Kawazoe, and P. Jena, Penta-graphene: A new carbon allotrope, *Proc. Natl. Acad. Sci. U.S.A.* 112(8), 2372 (2015)
51. J. W. Jiang, J. Leng, J. Li, Z. Guo, T. Chang, X. Guo, and T. Zhang, Twin graphene: A novel two-dimensional semiconducting carbon allotrope, *Carbon* 118, 370 (2017)
52. R. Baughman, H. Eckhardt, and M. Kertesz, Structure-property predictions for new planar forms of carbon: Layered phases containing sp^2 and *sp* atoms, *J. Chem. Phys.* 87(11), 6687 (1987)
53. Z. Wang, X. F. Zhou, X. Zhang, Q. Zhu, H. Dong, M. Zhao, and A. R. Oganov, Phagraphene: A low-energy graphene allotrope composed of 5–6–7 carbon rings with distorted Dirac cones, *Nano Lett.* 15(9), 6182 (2015)
54. F. Schlütter, T. Nishiuchi, V. Enkelmann, and K. Müllen, Octafunctionalized biphenylenes: Molecular precursors for isomeric graphene nanostructures, *Angew. Chem. Int. Ed.* 53(6), 1538 (2014)
55. C. X. Zhao, C. Y. Niu, Z. J. Qin, X. Y. Ren, J. T. Wang, J. H. Cho, and Y. Jia, H_{18} carbon: A new metallic phase with sp^2-sp^3 hybridized bonding network, *Sci. Rep.* 6(1), 21879 (2016)
56. Q. Song, B. Wang, K. Deng, X. Feng, M. Wagner, J. D. Gale, K. Müllen, and L. Zhi, Graphenylene, a unique two-dimensional carbon network with nondelocalized cyclohexatriene units, *J. Mater. Chem. C* 1(1), 38 (2013)
57. A. T. Koch, A. H. Khoshaman, H. D. Fan, G. A. Sawatzky, and A. Nojeh, Graphenylene Nanotubes, *J. Phys. Chem. Lett.* 6(19), 3982 (2015)
58. L. Zhu, Y. Jin, Q. Xue, X. Li, H. Zheng, T. Wu, and C. Ling, Theoretical study of a tunable and strain-controlled nanoporous graphenylene membrane for multifunctional gas separation, *J. Mater. Chem. A* 4(39), 15015 (2016)
59. W. Liu, M. Miao, and J. y. Liu, Band gap engineering of graphenylene by hydrogenation and halogenation: A density functional theory study, *RSC Advances* 5(87), 70766 (2015)
60. G. Fabris, N. Marana, E. Longo, and J. Sambrano, Theoretical study of porous surfaces derived from graphene and boron nitride, *J. Solid State Chem.* 258, 247 (2018)
61. Y. Qu, F. Li, and M. Zhao, Efficient ^{3}He/^{4}He separation in a nanoporous graphenylene membrane, *Phys. Chem. Chem. Phys.* 19(32), 21522 (2017)
62. A. Balaban, C. C. Rentia, and E. Ciupitu, Estimation of relative stability of several planar and tridimensional lattices for elementary carbon, *Rev. Roum. Chim.* 13, 231 (1968)
63. Q. S. Du, P. D. Tang, H. L. Huang, F. L. Du, K. Huang, N. Z. Xie, S. Y. Long, Y. M. Li, J. S. Qiu, and R. B. Huang, A new type of two-dimensional carbon crystal prepared from 1, 3, 5-trihydroxybenzene, *Sci. Rep.* 7(1), 40796 (2017)
64. R. Totani, C. Grazioli, T. Zhang, I. Bidermane, J. Lüder, M. de Simone, M. Coreno, B. Brena, L. Lozzi, and C. Puglia, Electronic structure investigation of biphenylene films, *J. Chem. Phys.* 146(5), 054705 (2017)
65. M. Bieri, M. Treier, J. Cai, K. Aït-Mansour, P. Ruffieux, O. Gröning, P. Gröning, M. Kastler, R. Rieger, X. Feng, K. Müllen, and R. Fasel, Porous graphenes: Two-dimensional polymer synthesis with atomic precision, *Chem. Commun.* 45(45), 6919 (2009)

66. Y. X. Yu, Graphenylene: A promising anode material for lithium-ion batteries with high mobility and storage, *J. Mater. Chem. A* 1(43), 13559 (2013)

67. S. Rouhi and A. Ghasemi, Investigation of the elastic properties of graphenylene using molecular dynamics simulations, *Mater. Res.* 20(1), 1 (2016)

68. H. Lu and S. D. Li, Two-dimensional carbon allotropes from graphene to graphyne, *J. Mater. Chem. C* 1(23), 3677 (2013)

69. G. Brunetto, P. Autreto, L. Machado, B. Santos, R. P. Dos Santos, and D. S. Galvao, Nonzero gap two-dimensional carbon allotrope from porous graphene, *J. Phys. Chem. C* 116(23), 12810 (2012)

70. M. De La Pierre, P. Karamanis, J. Baima, R. Orlando, C. Pouchan, and R. Dovesi, *Ab Initio* periodic simulation of the spectroscopic and optical properties of novel porous graphene phases, *J. Phys. Chem. C* 117(5), 2222 (2013)

71. G. S. Fabris, C. E. Junkermeier, and R. Paupitz, Porous graphene and graphenylene nanotubes: Electronic structure and strain effects, *Comput. Mater. Sci.* 140, 344 (2017)

72. M. Hankel and D. J. Searles, Lithium storage on carbon nitride, graphenylene and inorganic graphenylene, *Phys. Chem. Chem. Phys.* 18(21), 14205 (2016)

73. O. Rahaman, B. Mortazavi, A. Dianat, G. Cuniberti, and T. Rabczuk, Metamorphosis in carbon network: From penta-graphene to biphenylene under uniaxial tension, *FlatChem* 1, 65 (2017)

74. M. Q. Le, Mechanical properties of penta-graphene, hydrogenated penta-graphene, and penta-CN_2 sheets, *Comput. Mater. Sci.* 136, 181 (2017)

75. C. P. Ewels, X. Rocquefelte, H. W. Kroto, M. J. Rayson, P. R. Briddon, and M. I. Heggie, Predicting experimentally stable allotropes: Instability of penta-graphene, *Proc. Natl. Acad. Sci. USA* 112(51), 15609 (2015)

76. Z. Wang, F. Dong, B. Shen, R. Zhang, Y. Zheng, L. Chen, S. Wang, C. Wang, K. Ho, Y.-J. Fan, et al., Electronic and optical properties of novel carbon allotropes, *Carbon* 101, 77 (2016)

77. H. Einollahzadeh, R. Dariani, and S. Fazeli, Computing the band structure and energy gap of penta-graphene by using DFT and G0W0 approximations, *Solid State Commun.* 229, 1 (2016)

78. T. Stauber, J. Beltr'an, and J. Schliemann, Tight-binding approach to penta-graphene, *Sci. Rep.* 6(1), 22672 (2016)

79. X. Li, S. Zhang, F. Q. Wang, Y. Guo, J. Liu, and Q. Wang, Tuning the electronic and mechanical properties of penta-graphene via hydrogenation and fluorination, *Phys. Chem. Chem. Phys.* 18(21), 14191 (2016)

80. S. W. Cranford, When is 6 less than 5? Penta- to hexa-graphene transition, *Carbon* 96, 421 (2016)

81. H. Sun, S. Mukherjee, and C. V. Singh, Mechanical properties of monolayer penta-graphene and phagraphene: a first-principles study, *Phys. Chem. Chem. Phys.* 18(38), 26736 (2016)

82. Y. Zhang, Q. Pei, Z. Sha, Y. Zhang, and H. Gao, Remarkable enhancement in failure stress and strain of penta-graphene via chemical functionalization, *Nano Res.* 10(11), 3865 (2017)

83. S. Ebrahimi, Effect of hydrogen coverage on the buckling of penta-graphene by molecular dynamics simulation, *Mol. Simul.* 42(17), 1485 (2016)

84. Z. G. Yu and Y. W. Zhang, A comparative density functional study on electrical properties of layered penta-graphene, *J. Appl. Phys.* 118(16), 165706 (2015)

85. G. Berdiyorov, G. Dixit, and M. Madjet, Band gap engineering in penta-graphene by substitutional doping: first-principles calculations, *J. Phys.: Condens. Matter* 28(47), 475001 (2016)

86. J. Quijano-Briones, H. Fernández-Escamilla, and A. Tlahuice-Flores, Doped penta-graphene and hydrogenation of its related structures: a structural and electronic DFT-D study, *Phys. Chem. Chem. Phys.* 18(23), 15505 (2016)

87. G. R. Berdiyorov and M. E. A. Madjet, First-principles study of electronic transport and optical properties of penta-graphene, penta-SiC_2 and penta-CN_2, *RSC Advances* 6(56), 50867 (2016)

88. J. I. G. Enriquez and A. R. C. Villagracia, Hydrogen adsorption on pristine, defected, and 3d-block transition metal-doped penta-graphene, *Int. J. Hydrogen Energy* 41(28), 12157 (2016)

89. H. Einollahzadeh, S. M. Fazeli, and R. S. Dariani, Studying the electronic and phononic structure of penta-graphane, *Sci. Technol. Adv. Mater.* 17(1), 610 (2016)

90. B. Rajbanshi, S. Sarkar, B. Mandal, and P. Sarkar, Energetic and electronic structure of penta-graphene nanoribbons, *Carbon* 100, 118 (2016)

91. P. Yuan, Z. Zhang, Z. Fan, and M. Qiu, Electronic structure and magnetic properties of penta-graphene nanoribbons, *Phys. Chem. Chem. Phys.* 19(14), 9528 (2017)

92. W. Xu, G. Zhang, and B. Li, Thermal conductivity of penta-graphene from molecular dynamics study, *J. Chem. Phys.* 143(15), 154703 (2015)

93. H. Liu, G. Qin, Y. Lin, and M. Hu, Disparate strain dependent thermal conductivity of two-dimensional penta-structures, *Nano Lett.* 16(6), 3831 (2016)

94. F. Q. Wang, J. Yu, Q. Wang, Y. Kawazoe, and P. Jena, Lattice thermal conductivity of penta-graphene, *Carbon* 105, 424 (2016)

95. X. Wu, V. Varshney, J. Lee, T. Zhang, J. L. Wohlwend, A. K. Roy, and T. Luo, Hydrogenation of penta-graphene leads to unexpected large improvement in thermal conductivity, *Nano Lett.* 16(6), 3925 (2016)

96. F. Q. Wang, J. Liu, X. Li, Q. Wang, and Y. Kawazoe, Weak interlayer dependence of lattice thermal conductivity on stacking thickness of penta-graphene, *Appl. Phys. Lett.* 111(19), 192102 (2017)

97. Y. Y. Zhang, Q. X. Pei, Y. Cheng, Y. W. Zhang, and X. Zhang, Thermal conductivity of penta-graphene: The role of chemical functionalization, *Comput. Mater. Sci.* 137, 195 (2017)

98. R. Krishnan, W. S. Su, and H. T. Chen, A new carbon allotrope: Penta-graphene as a metal-free catalyst for CO oxidation, *Carbon* 114, 465 (2017)

99. B. Xiao, Y.-C. Li, X.-F. Yu, and J.-B. Cheng, Penta-graphene: A promising anode material as the Li/Na-ion battery with both extremely high theoretical capacity and fast charge/discharge rate, *ACS Appl. Mater. Interfaces* 8, 35342 (2016)

100. Q. Lu, M. Arroyo, and R. Huang, Elastic bending modulus of monolayer graphene, *J. Phys. D Appl. Phys.* 42(10), 102002 (2009)

101. M. M. Haley, S. C. Brand, and J. J. Pak, Carbon networks based on dehydrobenzoannulenes: Synthesis of graphdiyne substructures, *Angew. Chem. Int. Ed. Engl.* 36(8), 836 (1997)

102. G. Li, Y. Li, H. Liu, Y. Guo, Y. Li, and D. Zhu, Architecture of graphdiyne nanoscale films, *Chem. Commun. (Camb.)* 46(19), 3256 (2010)

103. Y. Q. Zhang, N. Kepčija, M. Kleinschrodt, K. Diller, S. Fischer, A. C. Papageorgiou, F. Allegretti, J. Björk, S. Klyatskaya, F. Klappenberger, M. Ruben, and J. V. Barth, Homo-coupling of terminal alkynes on a noble metal surface, *Nat. Commun.* 3(1), 1286 (2012)

104. A. Ivanovskii, Graphynes and graphdyines, *Prog. Solid State Chem.* 41(1–2), 1 (2013)

105. Q. Peng, J. Crean, L. Han, S. Liu, X. Wen, S. De, and A. Dearden, New materials graphyne, graphdiyne, graphone, and graphane: Review of properties, synthesis, and application in nanotechnology, *Nanotechnol. Sci. Appl.* 7, 1 (2014)

106. Y. Li, L. Xu, H. Liu, and Y. Li, Graphdiyne and graphyne: From theoretical predictions to practical construction, *Chem. Soc. Rev.* 43(8), 2572 (2014)

107. Z. Chen, C. Molina-Jirón, S. Klyatskaya, F. Klappenberger, and M. Ruben, 1D and 2D graphdiynes: Recent advances on the synthesis at interfaces and potential nanotechnological applications, *Ann. Phys.* 529(11), 1700056 (2017)

108. F. Chang, L. Huang, Y. Li, C. Guo, and Q. Diao, A short review of synthesis of graphdiyne and its potential applications, *Int. J. Electrochem. Sci.* 12, 10348 (2017)

109. X. Zhang, M. Zhu, P. Chen, Y. Li, H. Liu, Y. Li, and M. Liu, Pristine graphdiyne-hybridized photocatalysts using graphene oxide as a dual-functional coupling reagent, *Phys. Chem. Chem. Phys.* 17(2), 1217 (2015)

110. H. Qi, P. Yu, Y. Wang, G. Han, H. Liu, Y. Yi, Y. Li, and L. Mao, Graphdiyne oxides as excellent substrate for electroless deposition of Pd clusters with high catalytic activity, *J. Am. Chem. Soc.* 137(16), 5260 (2015)

111. L. Sun, P. Jiang, H. Liu, D. Fan, J. Liang, J. Wei, L. Cheng, J. Zhang, and J. Shi, Graphdiyne: A two-dimensional thermoelectric material with high figure of merit, *Carbon* 90, 255 (2015)

112. N. Narita, S. Nagai, S. Suzuki, and K. Nakao, Optimized geometries and electronic structures of graphyne and its family, *Phys. Rev. B* 58(16), 11009 (1998)

113. H. Bai, Y. Zhu, W. Qiao, and Y. Huang, Structures, stabilities and electronic properties of graphdiyne nanoribbons, *RSC Advances* 1(5), 768 (2011)

114. S. W. Cranford and M. J. Buehler, Mechanical properties of graphyne, *Carbon* 49(13), 4111 (2011)

115. Y. Yang and X. Xu, Mechanical properties of graphyne and its family – A molecular dynamics investigation, *Comput. Mater. Sci.* 61, 83 (2012)

116. Q. Peng, W. Ji, and S. De, Mechanical properties of graphyne monolayers: a first-principles study, *Phys. Chem. Chem. Phys.* 14(38), 13385 (2012)

117. S. Ajori, R. Ansari, and M. Mirnezhad, Mechanical properties of defective g-graphyne using molecular dynamics simulations, *Mater. Sci. Eng. A* 561, 34 (2013)

118. S. Ma, M. Zhang, L. Sun, and K. Zhang, High-temperature behavior of monolayer graphyne and graphdiyne, *Carbon* 99, 547 (2016)

119. Q. Yue, S. Chang, J. Kang, S. Qin, and J. Li, Mechanical and electronic properties of graphyne and its family under elastic strain: Theoretical predictions, *J. Phys. Chem. C* 117(28), 14804 (2013)

120. S. W. Cranford, D. B. Brommer, and M. J. Buehler, Extended graphynes: simple scaling laws for stiffness, strength and fracture, *Nanoscale* 4(24), 7797 (2012)

121. Y. Y. Zhang, Q. X. Pei, and C. M. Wang, Mechanical properties of graphynes under tension: A molecular dynamics study, *Appl. Phys. Lett.* 101, 666 (2012)

122. Y. Pei, Mechanical properties of graphdiyne sheet, *Physica B* 407(22), 4436 (2012)

123. M. M. Haley, Synthesis and properties of annulenic subunits of graphyne and graphdiyne nanoarchitectures, *Pure Appl. Chem.* 80(3), 519 (2008)

124. G. Luo, X. Qian, H. Liu, R. Qin, J. Zhou, L. Li, Z. Gao, E. Wang, W. N. Mei, J. Lu, Y. Li, and S. Nagase, Quasiparticle energies and excitonic effects of the two-dimensional carbon allotrope graphdiyne: Theory and experiment, *Phys. Rev. B* 84(7), 075439 (2011)

125. Y. Jiao, A. Du, M. Hankel, Z. Zhu, V. Rudolph, and S. C. Smith, Graphdiyne: A versatile nanomaterial for electronics and hydrogen purification, *Chem. Commun.* 47(43), 11843 (2011)

126. G. M. Psofogiannakis and G. E. Froudakis, Computational prediction of new hydrocarbon materials: The hydrogenated forms of graphdiyne, *J. Phys. Chem. C* 116(36), 19211 (2012)

127. M. Long, L. Tang, D. Wang, Y. Li, and Z. Shuai, Electronic structure and carrier mobility in graphdiyne sheet and nanoribbons: Theoretical predictions, *ACS Nano* 5(4), 2593 (2011)

128. S. Jalili, F. Houshmand, and J. Schofield, Study of carrier mobility of tubular and planar graphdiyne, *Appl. Phys. A* 119(2), 571 (2015)

129. J. Xi, M. Long, L. Tang, D. Wang, and Z. Shuai, First-principles prediction of charge mobility in carbon and organic nanomaterials, *Nanoscale* 4(15), 4348 (2012)

130. H. J. Cui, X. L. Sheng, Q. B. Yan, Q. R. Zheng, and G. Su, Strain-induced Dirac cone-like electronic structures and semiconductor–semimetal transition in graphdiyne, *Phys. Chem. Chem. Phys.* 15(21), 8179 (2013)

131. K. Krishnamoorthy, S. Thangavel, J. C. Veetil, N. Raju, G. Venugopal, and S. J. Kim, Graphdiyne nanostructures as a new electrode material for electrochemical supercapacitors, *International Journal of Hydrogen Energy* 41, 1672 (2016)

132. K. Srinivasu and S. K. Ghosh, Graphyne and graphdiyne: Promising materials for nanoelectronics and energy storage applications, *J. Phys. Chem. C* 116(9), 5951 (2012)

133. C. Sun and D. J. Searles, Lithium storage on graphdiyne predicted by DFT calculations, *J. Phys. Chem. C* 116(50), 26222 (2012)

134. H. Zhang, Y. Xia, H. Bu, X. Wang, M. Zhang, Y. Luo, and M. Zhao, Graphdiyne: A promising anode material for lithium ion batteries with high capacity and rate capability, *J. Appl. Phys.* 113(4), 044309 (2013)

135. B. Jang, J. Koo, M. Park, H. Lee, J. Nam, Y. Kwon, and H. Lee, Graphdiyne as a high-capacity lithium ion battery anode material, *Appl. Phys. Lett.* 103(26), 263904 (2013)

136. S. Zhang, H. Du, J. He, C. Huang, H. Liu, G. Cui, and Y. Li, Nitrogen-doped graphdiyne applied for lithium-ion storage, *ACS Appl. Mater. Interfaces* 8, 8467 (2016)

137. H. Du, H. Yang, C. Huang, J. He, H. Liu, and Y. Li, Graphdiyne applied for lithium-ion capacitors displaying high power and energy densities, *Nano Energy* 22, 615 (2016)

138. S. Zhang, H. Liu, C. Huang, G. Cui, and Y. Li, Bulk graphdiyne powder applied for highly efficient lithium storage, *Chem. Commun.* 51(10), 1834 (2015)

139. C. Huang, S. Zhang, H. Liu, Y. Li, G. Cui, and Y. Li, Graphdiyne for high capacity and long-life lithium storage, *Nano Energy* 11, 481 (2015)

140. H. Yu, A. Du, Y. Song, and D. J. Searles, Graphyne and graphdiyne: Versatile catalysts for dehydrogenation of light metal complex hydrides, *J. Phys. Chem. C* 117(42), 21643 (2013)

141. R. Liu, H. Liu, Y. Li, Y. Yi, X. Shang, S. Zhang, X. Yu, S. Zhang, H. Cao, and G. Zhang, Nitrogen-doped graphdiyne as a metal-free catalyst for high-performance oxygen reduction reactions, *Nanoscale* 6(19), 11336 (2014)

142. J. Li, X. Gao, B. Liu, Q. Feng, X. B. Li, M. Y. Huang, Z. Liu, J. Zhang, C. H. Tung, and L. Z. Wu, Graphdiyne: A metal-free material as hole transfer layer to fabricate quantum dot-sensitized photocathodes for hydrogen production, *J. Am. Chem. Soc.* 138(12), 3954 (2016)

143. S. W. Cranford and M. J. Buehler, Selective hydrogen purification through graphdiyne under ambient temperature and pressure, *Nanoscale* 4(15), 4587 (2012)

144. L. F. C. Pereira, B. Mortazavi, M. Makaremi, and T. Rabczuk, Anisotropic thermal conductivity and mechanical properties of phagraphene: A molecular dynamics study, *RSC Advances* 6(63), 57773 (2016)

145. D. Wu, S. Wang, J. Yuan, B. Yang, and H. Chen, Modulation of the electronic and mechanical properties of phagraphene via hydrogenation and fluorination, *Phys. Chem. Chem. Phys.* 19(19), 11771 (2017)

146. A. Lopez-Bezanilla, Strain-mediated modification of phagraphene Dirac cones, *J. Phys. Chem. C* 120(30), 17101 (2016)

147. A. Luo, R. Hu, Z. Fan, H. Zhang, J. Yuan, C. Yang, and Z. Zhang, Electronic structure, carrier mobility and device properties for mixed-edge phagraphene nanoribbon by hetero-atom doping, *Org. Electron.* 51, 277 (2017)

148. Y. Liu, Z. Chen, L. Tong, J. Zhang, and D. Sun, Effect of edge-hydrogen passivation and nanometer size on the electronic properties of phagraphene ribbons, *Comput. Mater. Sci.* 117, 279 (2016)

149. P. Yuan, Z. Fan, and Z. Zhang, Magneto-electronic properties and carrier mobility in phagraphene nanoribbons: A theoretical prediction, *Carbon* 124, 228 (2017)

150. D. Ferguson, D. J. Searles, and M. Hankel, Biphenylene and phagraphene as lithium ion battery anode materials, *ACS Appl. Mater. Interfaces* 9, 20577 (2017)

151. W. C. Lothrop, Biphenylene, *J. Am. Chem. Soc.* 63(5), 1187 (1941)

152. N. Yedla, P. Gupta, T. Y. Ng, and K. Geethalakshmi, Effect of loading direction and defects on the strength and fracture behavior of biphenylene based graphene monolayer, *Mater. Chem. Phys.* 202, 127 (2017)

153. M. A. Hudspeth, B. W. Whitman, V. Barone, and J. E. Peralta, Electronic properties of the biphenylene sheet and its one-dimensional derivatives, *ACS Nano* 4(8), 4565 (2010)

154. P. A. Denis, Stability and electronic properties of biphenylene based functionalized nanoribbons and sheets, *J. Phys. Chem. C* 118(43), 24976 (2014)

155. S. Wang, Optical response and excitonic effects in graphene nanoribbons derived from biphenylene, *Mater. Lett.* 167, 258 (2016)

156. P. A. Denis and F. Iribarne, Hydrogen storage in doped biphenylene based sheets, *Comput. Theor. Chem.* 1062, 30 (2015)

157. J. Liu, T. Zhao, S. Zhang, and Q. Wang, A new metallic carbon allotrope with high stability and potential for lithium ion battery anode material, *Nano Energy* 38, 263 (2017)

158. Y. Cheng, R. Melnik, Y. Kawazoe, and B. Wen, Three dimensional metallic carbon from distorting sp^3-bond, *Crystal Growth and Design* 16, 1360 (2016)

159. Y. Liu, X. Jiang, J. Fu, and J. Zhao, New metallic carbon: Three dimensionally carbon allotropes comprising ultrathin diamond nanostripes, *Carbon* 126, 601 (2018)

160. X. L. Sheng, Q. B. Yan, F. Ye, Q. R. Zheng, and G. Su, T-carbon: A novel carbon allotrope, *Phys. Rev. Lett.* 106(15), 155703 (2011)

161. X. Wu, X. Shi, M. Yao, S. Liu, X. Yang, L. Zhu, T. Cui, and B. Liu, Superhard three-dimensional carbon with metallic conductivity, *Carbon* 123, 311 (2017)

162. Q. Wei, Q. Zhang, H. Yan, and M. Zhang, A new superhard carbon allotrope: Tetragonal C_{64}, *J. Mater. Sci.* 52(5), 2385 (2017)

163. J. Q. Wang, C. X. Zhao, C. Y. Niu, Q. Sun, and Y. Jia, C_{20} T-carbon: A novel superhard sp^3 carbon allotrope with large cavities, *J. Phys.: Condens. Matter* 28(47), 475402 (2016)

164. D. Pantea, S. Brochu, S. Thiboutot, G. Ampleman, and G. Scholz, A morphological investigation of soot produced by the detonation of munitions, *Chemosphere* 65(5), 821 (2006)

165. F. Mouhat and F. X. Coudert, Necessary and sufficient elastic stability conditions in various crystal systems, *Phys. Rev. B* 90(22), 224104 (2014)

166. P. Chen, F. Huang, and S. Yun, Characterization of the condensed carbon in detonation soot, *Carbon* 41(11), 2093 (2003)

167. X. Q. Chen, H. Niu, D. Li, and Y. Li, Modeling hardness of polycrystalline materials and bulk metallic glasses, *Intermetallics* 19(9), 1275 (2011)

168. F. Gao, J. He, E. Wu, S. Liu, D. Yu, D. Li, S. Zhang, and Y. Tian, Hardness of covalent crystals, *Phys. Rev. Lett.* 91(1), 015502 (2003)

169. L. C. Xu, X. J. Song, R. Z. Wang, Z. Yang, X. Y. Li, and H. Yan, Designing electronic anisotropy of three-dimensional carbon allotropes for the all-carbon device, *Appl. Phys. Lett.* 107(2), 021905 (2015)

170. J. Zhang, R. Wang, X. Zhu, A. Pan, C. Han, X. Li, Z. Dan, C. Ma, W. Wang, and H. Su, Pseudo-topotactic conversion of carbon nanotubes to T-carbon nanowires under picosecond laser irradiation in methanol, *Nat. Commun.* 8(1), 683(2017)

171. X. Q. Chen, H. Niu, C. Franchini, D. Li, and Y. Li, Hardness of T-carbon: Density functional theory calculations, *Phys. Rev. B* 84(12), 121405 (2011)

172. S. Y. Yue, G. Qin, X. Zhang, X. Sheng, G. Su, and M. Hu, Thermal transport in novel carbon allotropes with sp^2 or sp^3 hybridization: An *ab initio* study, *Phys. Rev. B* 95(8), 085207 (2017)

173. Z. Wu, E. Zhao, H. Xiang, X. Hao, X. Liu, and J. Meng, Crystal structures and elastic properties of superhard IrN_2 and IrN_3 from first principles, *Phys. Rev. B* 76(5), 054115 (2007)

174. A. O. Lyakhov and A. R. Oganov, Evolutionary search for superhard materials: Methodology and applications to forms of carbon and TiO_2, *Phys. Rev. B* 84(9), 092130 (2011)

175. S. F. Pugh, XCII. Relations between the elastic moduli and the plastic properties of polycrystalline pure metals, *Philos. Mag.* 45(367), 823 (1954)

176. Y. Li, L. Xu, H. Liu, and Y. Li, Graphdiyne and graphyne: From theoretical predictions to practical construction, *Chem. Soc. Rev.* 43(8), 2572 (2014)

177. J. Kang, J. Li, F. Wu, S. S. Li, and J. B. Xia, Elastic, electronic, and optical properties of two-dimensional graphyne sheet, *J. Phys. Chem. C* 115(42), 20466 (2011)

178. R. C. Andrew, R. E. Mapasha, A. M. Ukpong, and N. Chetty, Mechanical properties of graphene and boronitrene, *Phys. Rev. B* 85(12), 125428 (2012)

179. J. Zhou, K. Lv, Q. Wang, X. Chen, Q. Sun, and P. Jena, Electronic structures and bonding of graphyne sheet and its BN analog, *J. Chem. Phys.* 134(17), 174701 (2011)

180. H. Bu, M. Zhao, H. Zhang, X. Wang, Y. Xi, and Z. Wang, Isoelectronic doping of graphdiyne with boron and nitrogen: Stable configurations and band gap modification, *J. Phys. Chem. A* 116(15), 3934 (2012)

181. C. Feng, X. H. Luan, P. Zhang, J. Xiao, D. G. Yang, and H. B. Qin, in: Electronic Packaging Technology (ICEPT), 2017, 18th International Conference on (IEEE, 2017), pp 1138–1142

182. Z. Xu, X. Lv, J. Li, J. Chen, and Q. Liu, A promising anode material for sodium-ion battery with high capacity and high diffusion ability: Graphyne and graphdiyne, *RSC Advances* 6(30), 25594 (2016)

183. Y. Pan, C. Xie, M. Xiong, M. Ma, L. Liu, Z. Li, S. Zhang, G. Gao, Z. Zhao, Y. Tian, B. Xu, and J. He, A superhard sp^3 microporous carbon with direct bandgap, *Chem. Phys. Lett.* 689, 68 (2017)

184. R. L. Austman, J. S. Milner, D. W. Holdsworth, and C. E. Dunning, The effect of the density–modulus relationship selected to apply material properties in a finite element model of long bone, *J. Biomech.* 41(15), 3171 (2008)